Taylor & Francis
Taylor & Francis Group

ORIGINAL ARTICLE

Effects of LET on oxygen-dependent and-independent generation of hydrogen peroxide in water irradiated by carbon-ion beams

Ken-ichiro Matsumoto[a], Megumi Ueno[a], Minako Nyui[a], Yoshimi Shoji[a,b] and Ikuo Nakanishi[b]

[a]Quantitative RedOx Sensing Group, Department of Radiation Regulatory Science Research, National Institute of Radiological Sciences, Quantum Life and Medical Science Directorate, National Institutes for Quantum and Radiological Science and Technology, Chiba-shi, Chiba, Japan; [b]Quantum RedOx Chemistry Group, Institute for Quantum Life Science, Quantum Life and Medical Science Directorate, National Institutes for Quantum and Radiological Science and Technology, Chiba-shi, Chiba, Japan

ABSTRACT

Linear energy transfer (LET) dependence of yields of O_2-dependent and O_2-independent hydrogen peroxide (H_2O_2) in water irradiated by ionizing radiation was investigated. The radiation-induced hydroxyl radical ($\bullet OH$) generation in an aqueous solution was reported to occur in two different localization densities, the milli-molar (relatively sparse) and/or molar (markedly-dense) levels. In the milli-molar-level $\bullet OH$ generation atmosphere, $\bullet OH$ generated at a molecular distance of ~ 7 nm are likely unable to interact. However, in the molar-level $\bullet OH$ generation atmosphere, several $\bullet OH$ were generated with a molecular distance of 1 nm or less, and two $\bullet OH$ can react to directly make H_2O_2. An aliquot of ultra-pure water was irradiated by 290-MeV/nucleon carbon-ion beams at the Heavy-Ion Medical Accelerator in Chiba (HIMAC, NIRS/QST, Chiba, Japan). Irradiation experiments were performed under aerobic or hypoxic ($<0.5\%$ oxygen) conditions, and several LET conditions (13, 20, 40, 60, 80, or >100 keV/μm). H_2O_2 generation in irradiated samples was estimated by three methods. The amount of H_2O_2 generated per dose was estimated and compared. O_2-independent H_2O_2 generation, i.e. H_2O_2 generation under hypoxic conditions, increased with increasing LET. On the other hand, the O_2-dependent H_2O_2 generation, i.e. subtraction of H_2O_2 generation under hypoxic conditions from H_2O_2 generation under aerobic conditions, decreased with increasing LET. This suggests that the markedly-dense $\bullet OH$ generation is positively correlated with LET. High-LET beams generate H_2O_2 in an oxygen-independent manner.

Introduction

The biological effects of ionizing radiation are induced by two different mechanisms, direct action and indirect action [1–3]. Direct action starts from direct ionization/ excitation of a biologically important molecule by ionizing radiation. Indirect action starts from a chemical reaction of a biological molecule with reactive species, such as reactive oxygen species (ROS) or other free radical species, generated via water radiolysis [4]. As ionizing radiation does not discriminate among molecular interactions, the ratio of direct and indirect action is determined by the volume ratio of target molecules. Ionizing radiation interacts with water molecules, which account for approximately 70% of the weight of living

organisms, at a higher rate than other molecules. Thus, roughly 70% of the biological effects of ionizing radiation are generally considered to be due to indirect action mediated by ROS and/or other reactive species.

In a precise sense, the ratio of direct and indirect reactions may be decided depending on the micro-/ nano-environment in the cell. Water molecules in the cytoplasm are held in a lattice/grid or reticulate structure made of proteins, similar to jelly. In the nucleus, DNA is wound-up and packed closely, and there is less water, which may be hydrate water. In the membrane structure, almost no water exists. Therefore, the ratio of direct and indirect reactions may depend on the density of biological molecules. In addition, the type of ROS that acts as the main player in such micro/nano-

Figure 1. Schematic drawing of the sample preparation for irradiation under hypoxic conditions. An aliquot (300–350 μL) of sample solution was sealed in an O_2-permeable polyethylene bag using a heat sealer. The samples were moved into a glove box, and then N_2 gas was pumped into the glove box to create a 0.5% or less O_2 atmosphere. The PTFE tubing or polyethylene bag containing the sample solution was again sealed in an O_2-impermeable bag with an O_2-absorber and colorimetric O_2-indicator.

environments in the cell is an important factor for determining the ratio of direct actions to indirect actions. The chemical reactivity and physical properties, such as membrane permeability, are different depending on the ROS.

A water molecule can be ionized (Equations (1–4)) or excited (Equation (5)) by ionizing radiation, and then generate hydroxyl radicals (•OH), hydrogen radicals (•H), hydrated electrons (e^-_{aq}), and other ions [5,6]:

$$H_2O \rightarrow H_2O^{\bullet+} + e^- \tag{1}$$

$$H_2O^{\bullet+} \rightarrow \bullet OH + H^+ \tag{2}$$

$$e^- + nH_2O \rightarrow e^-_{aq} \tag{3}$$

$$H^+ + e^-_{aq} \rightarrow \bullet H \tag{4}$$

$$H_2O^* \rightarrow \bullet OH + \bullet H \tag{5}$$
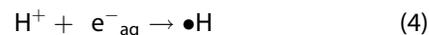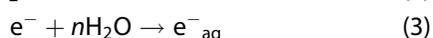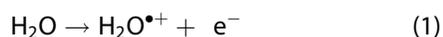
The •OH are a chemically short-lived free radical species, generally recognized as the most reactive attacker among ROS. The radiation-induced •OH in an aqueous solution were reported to be generated in two different locations at the milli-molar (relatively sparse) and/or molar (markedly dense) levels [7–9]. On the other hand, •H is likely given by reacting e^-_{aq} with hydrogen ion (H^+) (Equation (2)) or generated from excited water simultaneously with •OH (Equation (5)).

At the location of relatively sparse •OH generation, •OH generated at a molecular distance of ∼7 nm are likely unable to interact during their markedly short lifetime. Instead, •H can react with dissolved oxygen (O_2) to generate hydroperoxyl radicals ($HO_2^{\bullet}$) (Equation (6)).

$$\bullet H + O_2 \rightarrow HO_2^{\bullet} \tag{6}$$
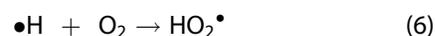
Then, a pair of $HO_2^{\bullet}$ molecules can react to generate H_2O_2 and O_2 (Equation (7)).

$$HO_2^{\bullet} + HO_2^{\bullet} \rightarrow H_2O_2 + O_2 \tag{7}$$
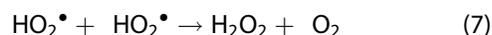
One H_2O_2 molecule is generated by consuming one O_2 molecule. Thus, O_2-dependent H_2O_2 generation can be an index of such sparse ionization.

At the location of markedly dense •OH generation, several •OH are generated with a molecular distance of 1 nm or less, and two or more •OH can react to directly make H_2O_2. H_2O_2 can be generated O_2-independently by the reaction of a pair of •OH (Equation (8)).

$$\bullet OH + \bullet OH \rightarrow H_2O_2 \tag{8}$$
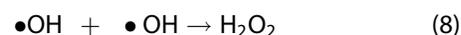
In such markedly dense •OH conditions, the H_2O_2 can react with another •OH and may yield hydroperoxyl radicals ($HO_2^{\bullet}$) (Equation (9)).

$$H_2O_2 + \bullet OH \rightarrow H_2O + HO_2^{\bullet} \tag{9}$$
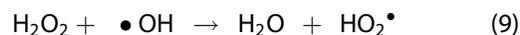
Then, a pair of $HO_2^{\bullet}$ molecules can react to again generate H_2O_2 and O_2 (Equation (7)). Ratios of the relatively sparse •OH yields to the total •OH yields decreased with increasing LET [7,9]. Therefore, there will be markedly dense generation at the principal location of •OH generation by higher LET beams. Indeed, O_2 consumption decreased with increasing LET [9,10]. Previous reports [7,9,10] suggested that O_2-independent H_2O_2 generation increases with increasing LET.

Carbon-ion beams have a track structure consisting of a core region, which is formed by linear dense ionization caused by primary particles and the penumbra region, which is branched ionization tracks formed by secondary electrons [11]. Therefore, O_2-dependent and -independent formation of H_2O_2 is expected in the penumbra and core regions, respectively. In addition, the

ratio of the O_2-dependent and -independent formation of H_2O_2 may be an index of the ratio of relatively sparse and markedly dense ionization/excitation. In this study, LET dependence of the O_2-independent H_2O_2 formation in water during carbon-ion beam irradiation was measured experimentally under hypoxic conditions. The LET dependence of the O_2-dependent and O_2-independent formation of H_2O_2 was compared.

Materials and methods

Chemicals

5,5-Dimethyl-1-pyrroline-N-oxide (DMPO) was purchased from Dojindo Laboratories, Ltd. (Kumamoto, Japan). H_2O_2 solution (30%) was purchased from FUJIFILM Wako Pure Chemical Corporation (Osaka, Japan). Other chemicals were of analytical grade. Deionized water (deionization by the Milli-Q system, Merck Millipore, Billerica, MA) was used for all experiments.

Preparation of samples for irradiation under aerobic or hypoxic conditions

Irradiation experiments were performed under aerobic or hypoxic (<0.5% oxygen) conditions. For irradiation under aerobic conditions, an aliquot of sample solution, i.e. 350 μL of milli-Q water, was placed into a polyethylene micro tube for X-ray irradiation or a polyethylene bag for carbon-ion beam irradiation. For both X-ray and carbon-beam irradiation under hypoxic conditions, milli-Q water was sealed in an O_2-permeable polyethylene bag. The samples for hypoxic experiments were moved into a glove box, and then N_2 gas was pumped into the glove box to create a 0.5% or less O_2 atmosphere. The polyethylene bag containing the sample solution was again sealed in an O_2-impermeable bag with an O_2-absorber and colorimetric O_2-indicator (Figure 1). The O_2-impermeable bag, O_2-absorber, and O_2-indicator were purchased from I.S.O. Inc. (Yokohama, Japan). The O_2-indicator remains pink in a hypoxic (<0.5% O_2) atmosphere and changes to bluish-violet when it detects oxygen. The change in color of the O_2-indicator is reversible.

X-ray irradiation

The reaction mixture in the polyethylene tube or bag was irradiated by 64 Gy of X-rays using PANTAK 320S (Shimadzu, Kyoto, Japan) at room temperature. The effective energy was 80 keV under the following conditions: X-ray tube voltage was 200 kV, X-ray tube current was 20 mA, and the thickness and materials of the pre-filter were 0.5-mm copper and 0.5-mm aluminum. The dose rate of X-ray irradiation was 3.04–3.15 Gy/min when the distance between the X-ray tube and the sample was 280 mm.

Carbon-ion beam irradiation

The polyethylene bag containing the reaction mixture was attached to a flat acrylic sample holder and irradiated by 64 Gy of 290-MeV/nucleon carbon-ion beams using the Heavy-Ion Medical Accelerator in Chiba (HIMAC, National Institute of Radiological Sciences, Chiba, Japan) at room temperature. Irradiation was performed using several LET conditions (13, 20, 40, 60, 80, or over 100 keV/μm). The calculated LET at the surface of the sample was based on the thickness of the binary filter and the polyethylene bag wall. The dose was planned at the surface of the sample and the dose rates varied depending on the LET.

Quantification of H_2O_2 generated in an irradiated water sample

H_2O_2 generation in irradiated water samples was estimated by the UV method proposed in this paper to simplify an experimental procedure and minimize variations in experimental conditions. For comparison, two other methods (see Appendix), the quinoid-dye method and Fenton method, were performed to confirm the reproducibility.

UV method: The •OH synthesized from H_2O_2 under the UVB irradiation were spin-trapped with DMPO, and the •OH adduct of DMPO (DMPO-OH) was then measured as an index of H_2O_2 using the X-band electron paramagnetic resonance (EPR) spectrometer. A 90-μl aliquot of irradiated water sample was placed into a micro tube, and 10 μL of 1 M DMPO water solution was added and mixed. The water sample was irradiated with UVB (12,000 μW/cm^2) for 5 min. Immediately after UVB irradiation, the water sample was drawn into PTFE (i.d. 0.32 ± 0.001 inches, wall 0.002 ± 0.0005 inches; ZEUS, Orangeburg, SC) tubing and measured using the X-band EPR. X-band EPR spectra were measured repeatedly 13 times every 30 s, and the average intensity of 13 measurements was recorded. The amount of H_2O_2 generated per dose was estimated using a standard curve previously prepared using a series of H_2O_2 water solutions of known concentrations (4.9–29.4 μM).

X-band EPR measurement

The PTFE tubing containing an aliquot of sample solution was placed in the TE mode cavity using a special
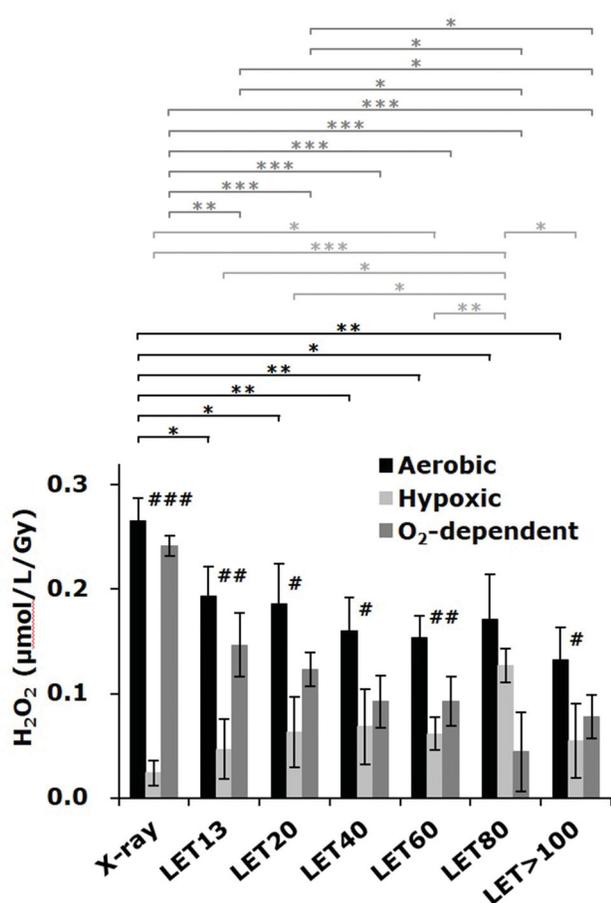
Figure 2. Carbon-ion beam induced H_2O_2 in water obtained by the UV method. The columns and the error bars indicate the average and SD of three experiments. Each experiment was carried out with triplicate measurements of aerobic and hypoxic samples. The O_2-dependent H_2O_2 yield, which was the difference between averages of aerobic and hypoxic samples, was calculated in each experiment and averaged among three experiments. #, ##, and ### indicate significance between aerobic and hypoxic conditions with $p < 0.05$, $p < 0.01$, and $p < 0.001$, respectively. *, **, and *** indicate significance between the different LET conditions with $p < 0.05$, $p < 0.01$, and $p < 0.001$, respectively.

sample holder and measured using the X-band EPR spectrometer (JEOL, Tokyo Japan). EPR data acquisition was controlled by the WIN-RAD ESR Data Analyzer System (Radical Research, Inc., Hino, Tokyo). The second line from the lower field of four lines of DMPO-OH was scanned. EPR spectra were measured under the following conditions: microwave frequency: 9.45 GHz, microwave power: 2 mW, lower magnetic field: 335.5 mT, field sweep width: +0.75 mT, field sweep resolution: 1024 points, sweep time: 15 s, time constant: 0.01 s, field modulation frequency: 100 kHz, and field modulation width: 0.063 mT. The acquired EPR spectra were analyzed using an in-house line fitting program and the Gaussian line shape was fitted. The signal height and

line width of the fitted Gaussian line were measured, and the EPR signal intensity was calculated as (signal height) $\times$ (line width)^2.

Statistical analysis

Significant differences between values for comparison were estimated using the TTEST function in Microsoft Excel 2010. Suitable "tail" and "type" for the TTEST function were selected as follows: The "tail" was 2 (two-tailed distribution) for stability tests because the difference between the two data groups was compared simply. The "type" was 2 (equal variance) or 3 (unequal variance), which was estimated using the FTEST function, and Student's or Welch's t-test was performed according to the "type." Grades of significance were estimated by $p < 0.05$, $p < 0.01$, and $p < 0.001$.

Results and discussion

The results of quantification of radiation-induced H_2O_2 in water under aerobic or hypoxic conditions obtained by the UV method are shown in Figure 2. Under aerobic conditions, the yield of H_2O_2 decreased with increasing LET, consistent with a previous report [9]. However, the yield of H_2O_2 under hypoxic conditions increased with increasing LET, peaking at LET = 80 keV/μm. The H_2O_2 detected in the sample irradiated under the hypoxic conditions was generated O_2-independently. The H_2O_2 detected in the sample irradiated under the aerobic conditions was the total of O_2-independent and -dependent generation. Therefore, the difference in the yield of H_2O_2 under aerobic conditions from that under hypoxic conditions is the yield of O_2-dependent H_2O_2. The yield of O_2-dependent H_2O_2 decreased with increasing LET. Reduced H_2O_2 yields under aerobic conditions, i.e. the total of O_2-independent and -dependent H_2O_2, were due to the LET dependency of O_2-dependent H_2O_2 generation.

It was previously reported that the O_2 consumption in the aerobic aqueous sample irradiated by X-rays or carbon-ion beams under several LET conditions decreased with increasing LET [9]. For example, the H_2O_2 yields in water under aerobic conditions estimated in a previous study [9], which were quantified by the Fenton method (see Appendix in the current paper), were 0.26, 0.20, and 0.17 μmol/L/Gy for X-rays, 20-keV/μm carbon-ion beams, and 80-keV/μm carbon-ion beams, respectively. These values were similar to those observed by the UV method in the current study. As described in the Appendix, however, values observed by the Fenton method and/or quinoid-dye

method exhibited relatively large variability among experiments. The LET-dependence of H_2O_2 yields was almost the same by all methods.

Furthermore, it was previously reported that the ratio of the yield of H_2O_2 to the O_2 consumption in the aqueous sample increased with increasing LET [9]. Oxygen consumption was estimated to be 0.41, 0.39, and 0.15 μmol/L/Gy for X-rays, 20-keV/μm carbon-ion beams, and 80-keV/μm carbon-ion beams, respectively. The ratios of H_2O_2 generation to oxygen consumption were 0.63, 0.51, and 1.13, for X-rays, 20-keV/μm carbon-ion beams, and 80-keV/μm carbon-ion beams, respectively. This suggests that O_2-independent H_2O_2 generation increases with higher LET irradiation. To confirm this prediction in the previous study experimentally, the H_2O_2 yields by X-ray or carbon-ion beam irradiation under hypoxic conditions were measured in the current study, which demonstrated that O_2-independent H_2O_2 generation, i.e. H_2O_2 yields under hypoxic conditions, is positively correlated with LET.

The H_2O_2 generation under hypoxic conditions likely results from the direct reaction between •OH based on Equation (8) or a combination of Equations (9) and (7) in an initially generated dense •OH cluster. Therefore, the O_2-independent H_2O_2 generation is an index of dense •OH generation, which simultaneously suggests dense ionization. The suppression of O_2-dependent H_2O_2 generation, which is based on Equations (6) and (7), with increasing LET suggested that sparse ionization is suppressed by increasing LET. Such sparse ionization expected for lower LET radiation may be causing sparse •H and •OH generation, and may lead to greater effects of radiation on oxygen through O_2-dependent $HO_2^{\bullet}$ and/or H_2O_2 generation. Relatively stable and membrane permeable H_2O_2 can travel longer distances and may have a higher chance of reaching itself at a biological target molecule in a cell.

O_2-independent H_2O_2 generation may be important *in vivo*. The tissue O_2 concentration, even in healthy normoxic tissues, is lower than that in the air-equilibrated *in vitro* situation. The O_2 concentration in air-saturated water at 37 °C is 0.21 mM. Extracellular pO_2 levels in fat and muscle tissues of healthy mice were reported to be 20 mmHg and 40 mmHg [12], corresponding to 0.027 and 0.054 mM, respectively. In *in vivo* hypoxic environments, particularly in hypoxic tumors, it will be less than 5 mmHg [13] or 0.007 mM. Bubbling water with 1% O_2 can increase the oxygen concentration to around 0.01 mM in water at 37 °C. Higher H_2O_2 generation in such a low pO_2 environment may play a role in the high therapeutic performance of high LET radiation.

Conclusion

H_2O_2 generation under aerobic conditions, i.e. total H_2O_2 generation, decreased with increasing LET. H_2O_2 generation under hypoxic conditions, i.e. O_2-independent H_2O_2 generation, increased with increasing LET. The O_2-dependent H_2O_2 generation, i.e. subtraction of H_2O_2 generation under hypoxic conditions from that under aerobic conditions, decreased with increasing LET. Higher LET beams can create more H_2O_2 in an O_2-independent manner than lower LET beams and/or photons. As the reaction of 2 •OH is required to generate H_2O_2 O_2-independently, this study suggests that O_2-independent H_2O_2 generation is an index of dense •OH, which produces an intermolecular distance of less than 1 nm. The dense •OH generation and sequential O_2-independent H_2O_2 generation are positively correlated with LET. In conclusion, this study demonstrated that the markedly dense ionization process of high LET radiation resulted in O_2-independent H_2O_2 generation.

Disclosure statement

No potential conflict of interest was reported by the authors.

Funding

References

[1] Hall EJ. Scientific view of low-level radiation risks. Radiographics. 1991;11(3):508–509.

[2] Goodhead DT. Mechanisms for the biological effectiveness of high-LET radiations. J Radiat Res. 1999;40: 1–13.

[3] Hirayama R, Ito A, Tomita M, et al. Contribution of direct and indirect actions in cell killing by high-LET radiation. Radiat Res. 2009;171(2):212–218.

[4] Alizadeh E, Sanz AG, Garcia G, et al. Radiation damage to DNA: the indirect effect of low energy electron. J Phys Chem Lett. 2013;4(5):820–825.

[5] Mitchell JB, DeGraff W, Kaufman D, et al. Inhibition of oxygen-dependent radiation-induced damage by the nitroxide superoxide dismutase mimic, tempol. Arch Biochem Biophys. 1991;289(1):62–70.

[6] Mitchell JB, Russo A, Kuppusamy P, et al. Radiation, radicals, and images. Ann N Y Acad Sci. 2000;899: 28–43.

[7] Matsumoto K, Ueno M, Nakanishi I, et al. Density of hydroxyl radicals generated in an aqueous solution by irradiating carbon-ion beam. Chem Pharm Bull. 2015; 63(3):195–199.

[8]   Ogawa Y, Sekine-Suzuki E, Ueno M, et al. Localized hydroxyl radical generation at mmol/l and mol/l levels in water by photon irradiation. J Clin Biochem Nutr. 2018;63(2):97–101.

[9]   Matsumoto K, Nyui M, Ueno M, et al. A quantitative analysis of carbon-ion beam-induced reactive oxygen species and redox reactions. J Clin Biochem Nutr. 2019;65(1):1–7.

[10]   Matsumoto K, Aoki I, Nakanishi I, et al. Distribution of hydrogen peroxide-dependent reaction in a gelatin sample irradiated by carbon ion beam. Magn Reson Med Sci. 2010;9(3):131–140.

[11]   Muroya Y, Plante I, Azzam EI, et al. High-LET ion radiolysis of water: visualization of the formation and evolution of ion tracks and relevance to the radiation-induced bystander effect. Radiat Res. 2006;165(4): 485–491.

[12]   Matsumoto A, Matsumoto S, Sowers AL, et al. Absolute oxygen tension (pO$_2$) in murine fatty and muscle tissue as determined by EPR. Magn Reson Med. 2005;54(6):1530–1535.

[13]   Kishimoto S, Krishna MC, Khramtsov VV, et al. *In vivo* application of proton-electron double-resonance imaging. Antioxid Redox Signal. 2018;28(15): 1345–1364.

[14]   Kasahara Y, Ashihara Y. Colorimetry of angiotensin-I converting enzyme activity in serum. Clin Chem. 1981; 27(11):1922–1925.

[15]   Ueda U, Matsumoto K, Endo K. Evidence of hepatic endogenous hydrogen peroxide in bile of selenium-deficient rat. Biochem Biophys Res Commun. 2000; 271(3):699–702.

[16]   Ui I, Okajo A, Endo K, et al. Effect of hydrogen peroxide in redox status estimation using nitroxyl spin probe. Free Radic Biol Med. 2004;37(12):2012–2017.

Appendix

Quantification of H$_2$O$_2$ generated in an irradiated water sample by alternative methods

Quinoid-dye method: The H$_2$O$_2$ concentration in the irradiated water samples was measured using the spectrophotometric method [14]. This method is based on measurement of a red quinoid dye formed by a reaction of 4-aminoantipyrine, phenol, and H$_2$O$_2$ under coexisting peroxidase. This quinoid dye can be detected by absorbance at 505 nm using a spectrophotometer.

Fenton method: The •OH synthesized from H$_2$O$_2$ under the presence of Fe^{2+} were spin-trapped with DMPO, and the •OH adduct of DMPO (DMPO-OH) was then measured as an index of H$_2$O$_2$ using the X-band EPR spectrometer [15, 16]. Irradiated water samples (160 μL) were placed in a micro tube and then 500 mmol/L DMPO (20 μL) was added. When 1.0 mmol/L FeSO$_4$ (20 μL) was added, the sample was immediately mixed, transferred to a 25-cm segment of PTFE tubing, and measured using the X-band EPR spectrometer within a minute of mixing. X-band EPR spectra were measured repeatedly 10 times every 30 s, and the maximum intensity among 10 measurements was recorded. The amount of H$_2$O$_2$ generated per dose was estimated using a standard curve previously prepared using a series of H$_2$O$_2$ water solutions of known concentrations (4.9–29.4 μM).

Standard curves for the quantification of H$_2$O$_2$ were obtained by three methods (Supplementary Figure 1). The relation between the H$_2$O$_2$ concentration in the sample solution and absorption of quinoid dye at 505 nm (Supplementary Figure 1(A)) or EPR signal intensity of DMPO-OH (Supplementary Figure 1(B,C)) was linear. Each standard curve was used for the corresponding experiment.

Although the three methods produced slightly different values, they were all similar (Supplementary Figure 2). The quinoid-dye method gave slightly higher values and the Fenton method gave slightly lower values than the UV method. The values obtained in this study using the quinoid-dye method were higher than those in a previous report [9], whereas those obtained by the Fenton method were lower [9]. These two methods had relatively large variations among individual experiments.

The values obtained by the quinoid-dye method were affected by reaction time and temperature. The enzymatic reaction of three compounds, i.e. phenol, 4-aminoantipyrine, and H$_2$O$_2$, is also affected by quality of peroxidase. Therefore, the standard curve for quantification should be remade for each experiment. This reaction may be good for biological samples, but it requires additional caution. The values obtained by the Fenton method depended largely on the concentration of Fe^{2+}. Relatively low concentrations of H$_2$O$_2$ in the sample water can be detected with good sensitivity, but FeSO$_4$ solution must be freshly prepared and the standard curve for quantification should be remade for each experiment. The values obtained by the UV method only depend on UVB irradiation time under a constant light intensity and the standard curve can be reused if the same lot of DMPO is used.
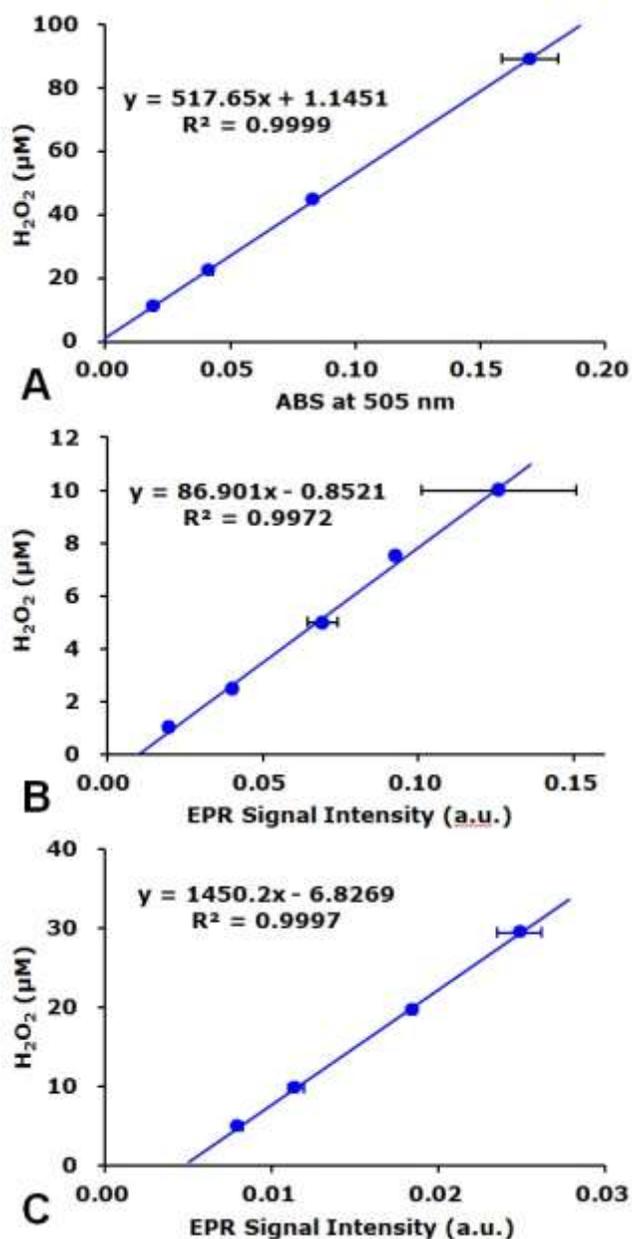
Suppl. Fig. 1. Standard curves for quantification of H_2O_2 obtained with each method. (A) Quinoid-dye method: Absorption of a red quinoid dye at 505 nm formed by the reaction of 4-aminoantipyrine, phenol, and H_2O_2 under coexisting peroxidase was measured. (B) Fenton method: The •OH synthesized from H_2O_2 in the presence of Fe^{2+} were spin-trapped with DMPO and the •OH adduct of DMPO (DMPO-OH) was measured using the X-band EPR spectrometer. (C) UV method: The •OH synthesized from H_2O_2 under UVB irradiation were spin-trapped with DMPO and the DMPO-OH was then measured using the X-band EPR spectrometer.
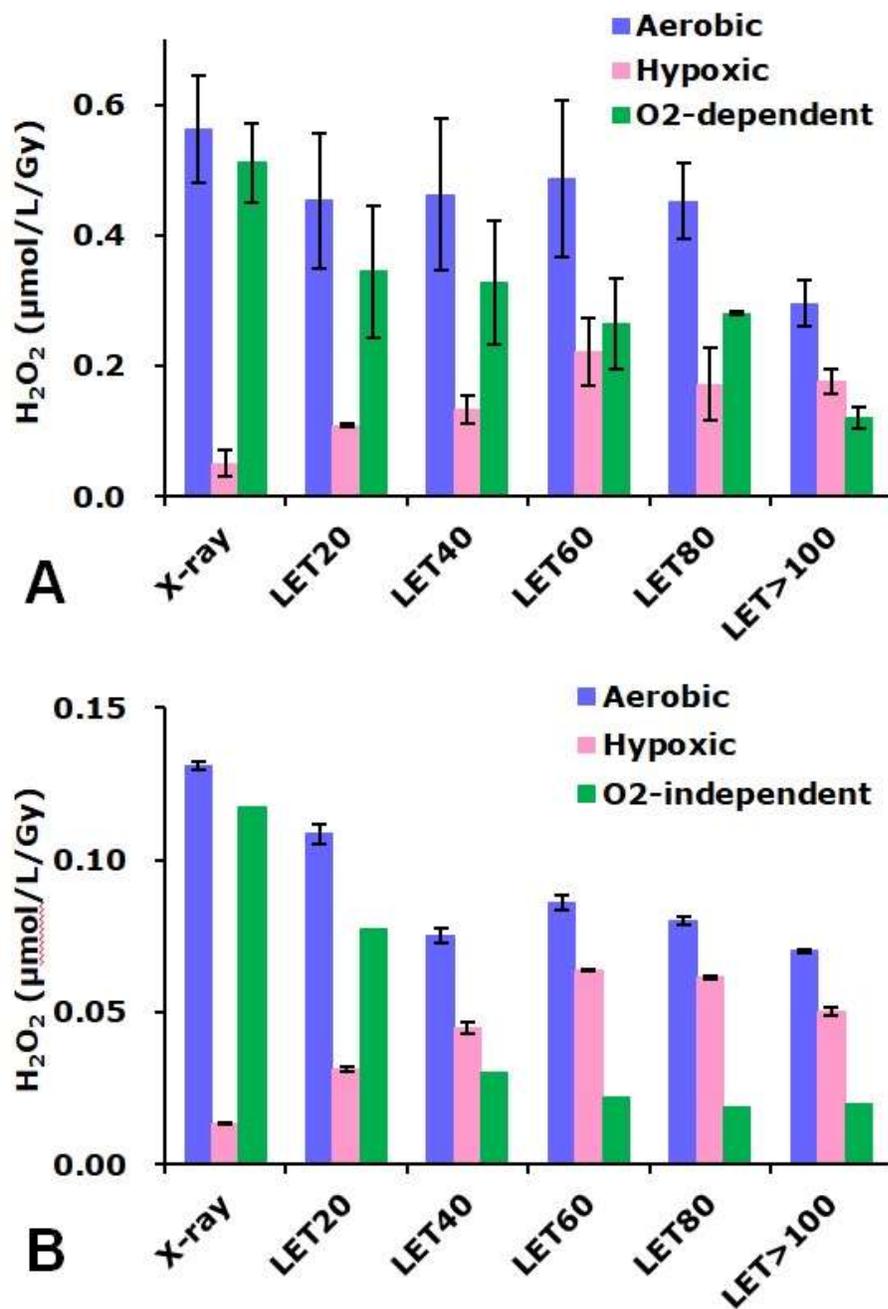
Suppl. Fig. 2.Carbon-ion-beam-induced H_2O_2 in water observed by the quinoid-dye method and the Fenton method. (A) The LET-dependent H_2O_2 yield under aerobic and hypoxic conditions was measured by the quinoid-dye method. The columns and the error bars indicate the average and SD of two experiments, and each experiment was carried out with triplicate measurements. (B) Results of a single experiment with the Fenton method are shown. The columns and error bars indicate the average and SD of three measurements.